CONFERENCE PRE-PRINT

IMPLEMENTATION OF A TIGHTLY BAFFLED LONG-LEGGED DIVERTOR IN TCV

H. REIMERDES, O. FÉVRIER, C. THEILER, H. ELAIAN, Y. ANDREBE, B. BROWN, R. DUCKER, G. DURR-LEGOUPIL-NICOUD, B.P. DUVAL, D. MYKYTCHUK, U. SHEIKH, P. SINTRE, E. TONELLO, B. VINCENT AND THE TCV TEAM*
École Polytechnique Fédérale de Lausanne (EPFL), Swiss Plasma Center (SPC), Lausanne, Switzerland
Email: holger.reimerdes@epfl.ch

Abstract

The TCV tokamak contributes to the development of nuclear fusion energy with proof-of-principle experiments and by validating models that are used to predict reactor performance. In the next upgrade of the TCV divertor it is planned to test a tightly baffled, long-legged divertor (TBLLD), a novel concept designed to enhance power exhaust handling with minimal modification to the magnetic configuration. The project is guided by simulations using the SOLPS-ITER code that indicate that a TBLLD can improve TCV's power exhaust capability by an order of magnitude compared to its unbaffled configuration. Tight baffling sustains a high poloidal neutral density gradient along the divertor leg, thereby increasing the neutral density in front of the divertor target and enhancing volumetric power dissipation. The simulations informed the design of a proof-of-principle TBLLD for the outer TCV divertor, while ensuring compatibility with high-power plasma scenarios. A straight, vertical design, that incorporates graphite baffle tiles and is built around TCV's reciprocating divertor probe array (RDPA), maintains engineering simplicity and enables sufficient diagnostic access. The resulting, more restrictive divertor, will also be accessible to poloidally distributed wall-mounted Langmuir probes, surface thermocouples, pressure gauges, and spectrometric lines of sight providing the measurements that will be sufficient to assess the TBLLD concept. A dedicated experimental campaign is planned for 2026.

1 INTRODUCTION

The 'Tokamak à Configuration Variable' (TCV) is a mid-size tokamak (major radius $R_0 = 0.88$ m, magnetic field on axis $B_0 \leq 1.54$ T) at the Swiss Plasma Center (SPC) in Lausanne. It contributes to the development of nuclear fusion energy through proof-of-principle experiments and by experimentally testing the theoretical models that are used to extrapolate existing solutions to a reactor [1]. As part of the Swiss Roadmap for Research Infrastructures, the SPC will augment TCV to test a tightly baffled, long-legged, divertor (TBLLD), a divertor concept [2] that promises to increase the power exhaust capability of a divertor with minor changes in the magnetic configuration from a conventional single-null divertor. Minimising changes in the magnetic configuration limits any additional engineering challenges and, hence, the high costs, commonly associated with alternative divertor solutions for fusion reactors [3]. For these reasons a TBLLD is, for example, among the divertor solutions being considered for the ARC reactor [4]. Tight baffling along the divertor leg hampers the movement of neutrals from the target to the main plasma and, thereby, leads to a higher neutral density poloidal gradient that promotes higher neutral densities in front of the target. A high fraction of the exhaust power then passes from the plasma to the neutrals before interacting with the divertor target. The close link between divertor neutral pressure and the power exhaust potential has been established empirically in tokamak experiments [5] and is seen in simulations, including those used to design the ITER divertor [6]. Edge plasma simulations using the SOLPS-ITER code [7] predict that a TBLLD in TCV can increase the divertor's power exhaust capability by up to an order of magnitude compared to its unbaffled configuration [8]. The TCV upgrade is structured in two phases with the first phase seeking a proof-of-principle test of the TBLLD concept. Upon successful demonstration of the TBLLD concept, a second phase aims to identify an optimised baffle geometry that also includes a solution for the inner divertor together with performant particle exhaust that remains compatible with an attractive core plasma scenario. The specifications for the proof-of-principle TBLLD are derived in Section 2. The chosen engineering implementation is presented in Section 3. The plans for a dedicated gas delivery systems are outlined in Section 4 and new, or modified, diagnostics required for the proof-of-principle are described in Section 5 before concluding in Section 6.

2 TBLLD SPECIFICATIONS

A proof-of principle of the TBLLD concept must demonstrate that tight baffling leads to a substantially higher poloidal gradient in the neutral pressure along the extended divertor leg. It must also show that this gradient leads to a substantial increase of the neutral pressure at the target and, consequently, a lower target plasma temperature than an unbaffled divertor for the same core scenario, i.e. the same plasma density, exhaust power and impurity

* *See author list of C. Theiler et al., "Progress and innovations in the TCV tokamak research programme", this conference.*

concentration inside the last-closed-flux-surface (LCFS). For simplicity this proof-of-principle will first be carried out only for the outer divertor. To demonstrate a substantial increase of the tolerable exhaust power, the gas baffles that form the TBLLD must be compatible with high power auxiliary heated TCV plasma configurations. The considered core scenarios include high power L- and H-modes, the latter with edge localised modes (ELMs) or quasi-continuous exhaust (QCE). While electron cyclotron resonance heating (ECRH) of L-modes does not unduly constrain the plasma position, neutral beam injection (NBI) heating, highly desirable for H-mode access, requires a plasma magnetic axis close to TCV's midplane, constraining the vertical extent of the TBLLD. Reliable NBI heated H-mode are routinely obtained with the magnetic axis 0.10 m above the midplane. Adopting a straight, vertical, TBLLD facilitates the engineering design and allows the continued use of TCV's reciprocating divertor probe array (RDPA) [9] along the outer divertor leg[†]. These constraints led to the choice of a baffled divertor leg length, L_{TBLLD}, of 0.335 m, Figure 1. This will allow for NBI heating injecting up to 1.3 MW in the plasma current direction (co-injection) and up to 2.6 MW in both directions, although not all the injected power will be deposited in the plasma. Higher absorbed heating power and, hence, a greater exhaust challenge will be obtained for low density ECRH heated plasmas, where up to 2.5 MW of power can be injected at the second harmonic with extraordinary mode absorption close to 100%. Infrared thermography, in such scenarios, has inferred parallel heat fluxes at the outer divertor entrance of up to 100 MW/m^2. The low plasma density required for the absorption of the microwaves increases the exhaust challenge further. Using a simple model for the impurity concentration required for acceptable target conditions, $c_z \sim \left(\frac{P_{\mathrm{sep}}B}{R}\right)/n_{e,sep}^2$, as a metric for the power exhaust challenge [10], these scenarios equal or exceed the challenge expected in reactors.

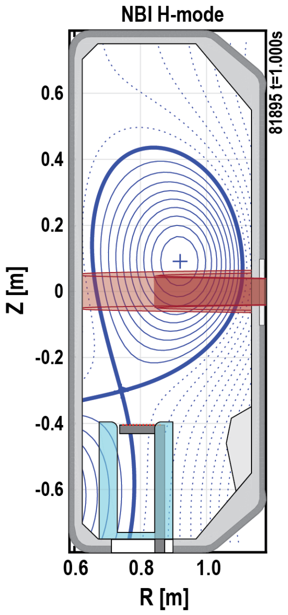

Figure 1. *Poloidal cross section of an NBI heated H-mode with a schematic of the heating beam profile (red) and the planned TBLLD contour (cyan) designed around TCV's RDPA (grey).*

The development of the specifications for the TBLLD width, W_{TBLLD}, i.e. the distance between the baffles, was guided by SOLPS-ITER simulations for TCV configurations with a tightly-baffled divertor of similar length to the planned divertor, over a range of widths [8]. A distance between the inner and outer baffle that corresponds to 10 heat flux fall-off lengths, λ_q, (referred to as TBLLD1 in [8]) is already found to significantly affect the power exhaust. The beneficial effect is predicted to increase as W_{TBLLD} is decreased to 6 λ_q (referred to as TBLLD2 in [8]). The beneficial effect of a further decrease of W_{TBLLD} is expected to be limited by the increasing recycling, and possibly excessive power loads, at the top of the TBLLD baffle tiles, but the employed version of SOLPS-ITER, which utilises a structured grid, did not allow to accurately predict this limit. Measured heat flux fall-off lengths of the targeted core scenarios, mapped to the outboard midplane, $\lambda_{q,u}$, vary from 1.5 mm in high current H-modes to 6 mm in low current, high power L-modes. Poloidal flux expansion, $f_{x,t}$, broadens the scrape-off layer (SOL) in the divertor. In TCV, $f_{x,t}$ can be varied from approximately 2 to 7, whilst maintaining the flux surface geometry parallel along the divertor leg, and to still higher values, if flaring towards the target is accepted. Assuming that the ratio of W_{TBLLD} and $\lambda_{q,t}$ is a good metric for TBLLD closure, flux expansion can be used to

[†] Note that the RDPA will be rotated by 180 Deg. with respect to its current installation for its boom to be on the low-field side of the TBLLD.

control plasma plugging in the TBLLD. A baffle distance of 0.113 m is chosen, Figure 1, to allow all considered core scenarios to be tested with a baffle distance of not more than 10 λ_q, Figure 2.

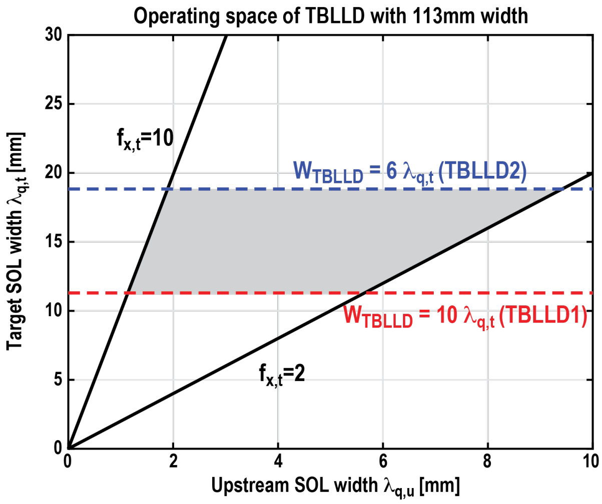

Figure 2. *Operating space of divertor closure for the range of attainable target flux expansions, $f_{x,t}$, and expected SOL widths, $\lambda_{q,u}$.*

The performance of the selected TBLLD dimensions were cross-checked with further SOLPS-ITER simulations [11]. The considered equilibrium has a plasma current of 250 kA and a flux expansion at the outer target, $f_{x,t}$, of 3.0. The strike point is placed at the centre of the TBLLD target and flux surfaces in the TBLLD volume are approximately vertical, i.e. conformal with the baffles, Figure 3(a). The simulations use standard transport coefficients and boundary conditions for TCV [11]. Drifts were neglected, and the fuelling adjusted to obtain an outboard midplane separatrix electron density, $n_{e,u}^{sep}$, of $1.5 \times 10^{10} m^{-3}$, as in the simulations that guided the design [8].

The planned TBLLD leads to the same peak outer target electron temperatures of 12 eV with more than 3x the assumed input power than in the unbaffled configuration, Figure3(b). Detachment in the TBLLD is compatible with 800kW crossing from the plasma core into the simulated edge region, P_{core}, inline with the performance TBLLD1 in [8] and, therefore, consistent with the design specifications.

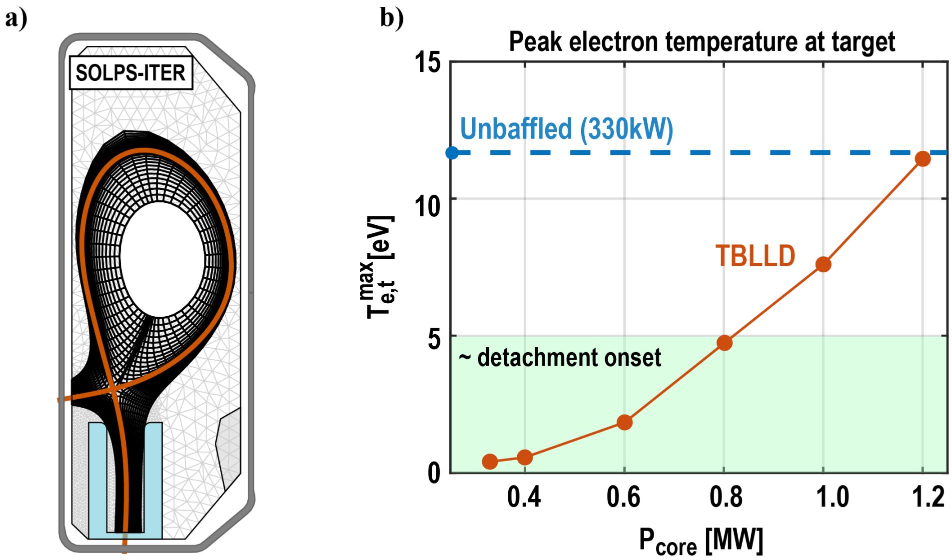

Figure 3. (a) SOLPS-ITER mesh of an equilibrium adopted for the TBLLD. (b) Dependence of the simulated peak electron temperatures at the outer target, $T_{e,t}^{max}$, on the assumed input power across the core simulation boundary, P_{core} (figure adopted from [11]).

3 TBLLD ENGINEERING DESIGN

The engineering design of the TBLLD is based on 64 inner and 64 outer baffle tiles, each, fabricated from the same high purity, polycrystalline graphite used for the TCV wall protection tiles, Figure 4(a). Each tile has a single attachment to steel plates that are attached to existing rails that are spot welded to the vacuum vessel, Figure 4(b). Ceramic inserts between baffle tiles at four toroidal locations are added to avoid the induction of toroidal currents. A radial tile depth of 55 mm is required for mechanical resilience to halo currents that can arise from vertical displacement events, similarly to the design criteria used for the first-generation TCV baffles [12].

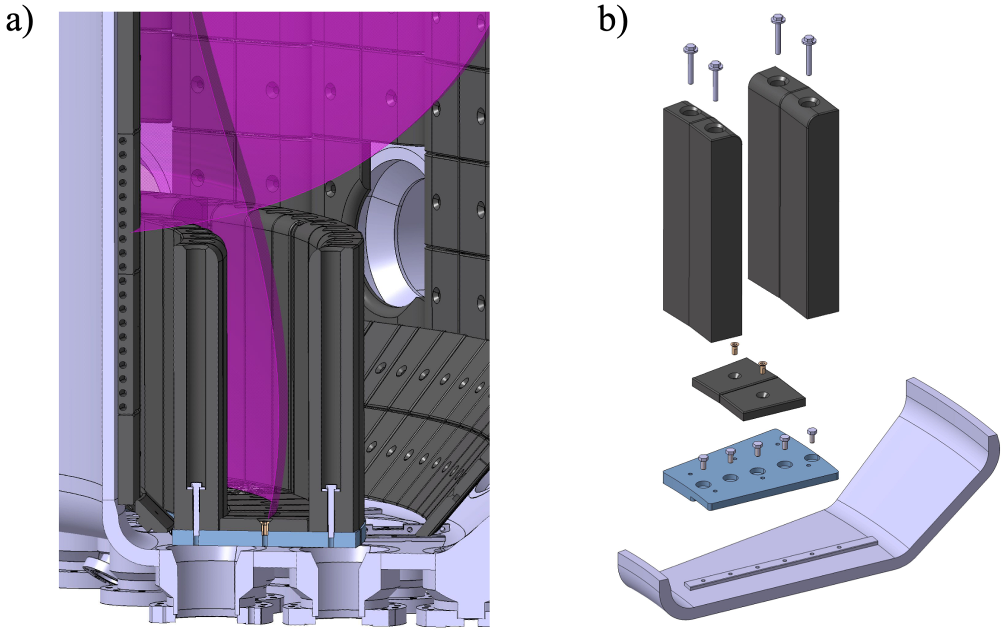

Figure 4. *CAD model of (a) the TBLLD arrangement in the TCV vessel and (b) a schematic of the attachment of the TBLLD graphite tiles (dark grey) via single screws to steel plates (blue), which are themselves attached to existing rails welded to the vacuum vessel (light grey).*

A proof-of-principle of the TBLLD concept requires establishing a high neutral density in the divertor. Neutral gas leakage through gaps in the baffles, typically described by a neutral conductance C_{leak}, must remain small compared to the flux of neutrals from the target to the baffle throat, C_{baffle}. Post-processing of the SOLPS-ITER calculation estimates that C_{baffle} of TBLLD2 in [8] is as low as 50 m^3/s [13]. The gas tightness of the planned baffles was analysed using kinetic modelling of the neutral gas, which limit the gaps between tiles to 0.5 mm, to reduce C_{leak} below 10 m^3/s. With higher gas tightness required compared to the first-generation baffles [14], no through openings for diagnostics are foreseen.

4 PARTICLE CONTROL

The TBLLD gas delivery system is designed for fuelling and impurity seeding at the outer divertor target. It consists of three gas lines that can provide different gases. The gas lines lead to one (lines #1 and #2) or three piezo valves (line #3), located at four toroidally equidistant locations placed at the centre of the TBLLD, Figure 5. This arrangement allows for the detection and investigation of potential toroidal asymmetries due to the discrete gas delivery locations. Individual gas valves can be used to vary the toroidal distance between the gas delivery location and diagnostics. If required, fuelling or impurity seeding can be administered from four equidistant valves. The system also allows simultaneously fuelling and seeding from two, toroidally opposed locations, each. The TBLLD gas delivery system is complemented by existing gas valves for fuelling and/or seeding at several poloidal locations that include the private flux region, the HFS SOL, the LFS SOL and from the top of the TCV vessel.

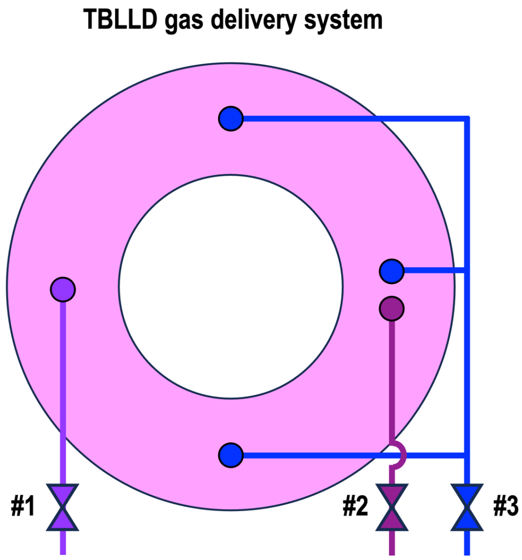

Figure 5. *Schematic of the gas delivery system's toroidal geometry with three gas lines and five piezo valves at four toroidal locations.*

The first phase of the TBLLD upgrade does not foresee additional provisions for pumping. As the effective pumping speed of TCV's four turbo-molecular pumps, which are connected through cylindrical ducts to lower lateral ports, is only 1.7 m^3/s [15], the dominant particle sink during plasma discharges will remain particle adsorption and absorption on the carbon surfaces of the plasma facing components.

5 DIAGNOSTICS

The divertor geometry without lateral baffle openings challenges diagnostic access to the divertor. Essential measurements to validate the TBLLD concept will include the neutral particle distribution along the divertor leg, target plasma particle and heat loads and the target plasma temperatures. Further, desirable, measurements are planned to characterise the divertor plasma along the divertor leg.

Measurements of the neutral particle distribution will be provided by a poloidal set of seven ASDEX-type pressure gauges (APGs) installed in the TBLLD tiles, Figure 6(a). These gauges are identical to existing gauges [16]. Each gauge connects to the TBLLD via a 70 mm long tube. A tube diameter of 7 mm guarantees that an isotropic neutral distribution reaches the gauge head [17]. The set includes three APGs located at different heights in the outer baffle to resolve poloidal pressure gradients. The APG measurements will be complemented by an existing MANTIS system [18] mounted in the midplane, from where, thanks to several locally modified outer baffle tiles[‡], it will have a near un-obstructed view into the TBLLD.

Measurements of target fluxes will be provided by tightly spaced, surface mounted, Langmuir probe arrays [19], Figure 6(b). A spacing of 7.5 mm at the target, 11 mm on the outer baffle and 20 mm on the inner baffle will be adequate to resolve target profiles as well as estimate cross-field transport to the baffles. Target heat fluxes are also measured by a set of eight surface eroding thermocouples [20], Figure 6(a), with several prototypes currently being qualified in TCV. Complementary information can be obtained from the vertical infrared (IR) thermography system [21], which images a large fraction of the TBLLD target. Its interpretation may, however, be complicated by plasma emission of the expected dense TBLLD divertor plasma in the IR wavelength range. Langmuir probes will provide essential information on the target electron temperature.

Further, desirable, measurements to characterise the divertor plasma along the divertor leg will be obtained by the RDPA [22], Figure 6(a). With its boom hidden in a recess in the outer baffle tiles, there should only remain limited perturbations to the divertor plasma with 10 of its original 12 Langmuir probes able to diagnose the entire TBLLD poloidal cross section. Passages from the RDPA port to the main chamber in the sub-divertor will be plugged by a steel structure to avoid neutral leakage. Spectroscopic information is obtained across horizontal lines-of-sight by the divertor spectrometer system (DSS) [23]. Eight equidistant radial LoSs, Figure 6(a), offer poloidal resolution. Optional connections to standard or high-resolution spectrometers allow trade-offs between spectral

[‡] The tile modifications are limited to the top of the baffles and have only a negligible effect on neutral gas leakage.

resolution and sampling frequency that will be used for a wide range of measurement techniques. Measurements of the C III triplet line emission at 465 nm will, for example, be used to track the effect of fast transients, such as ELMs, in the TBLLD. The radial LoSs are supplemented by six toroidally viewing LoSs at mid-height for radial resolution and parallel flow measurements [24]. Line-integrated information of the divertor electron density is provided along four vertical chords of TCV's interferometer [25] that pass through the TBLLD volume at different radii, Figure 7. As for the RDPA port, the interferometer port is isolated from the main chamber through steel plugs.

While the inner divertor is not the main objective of the first phase of the divertor upgrade, power redistribution from the tightly-baffled outer divertor to the conventional inner divertor may affect the evaluation of the TBLLD's performance. Preserving the ability to diagnose inner strike point particle and power loads with Langmuir probes and IR thermography, Figure 6(b), is, therefore, important. The Langmuir probe coverage of the inner target will even be augmented with respect to the current coverage to assist in this endeavour.

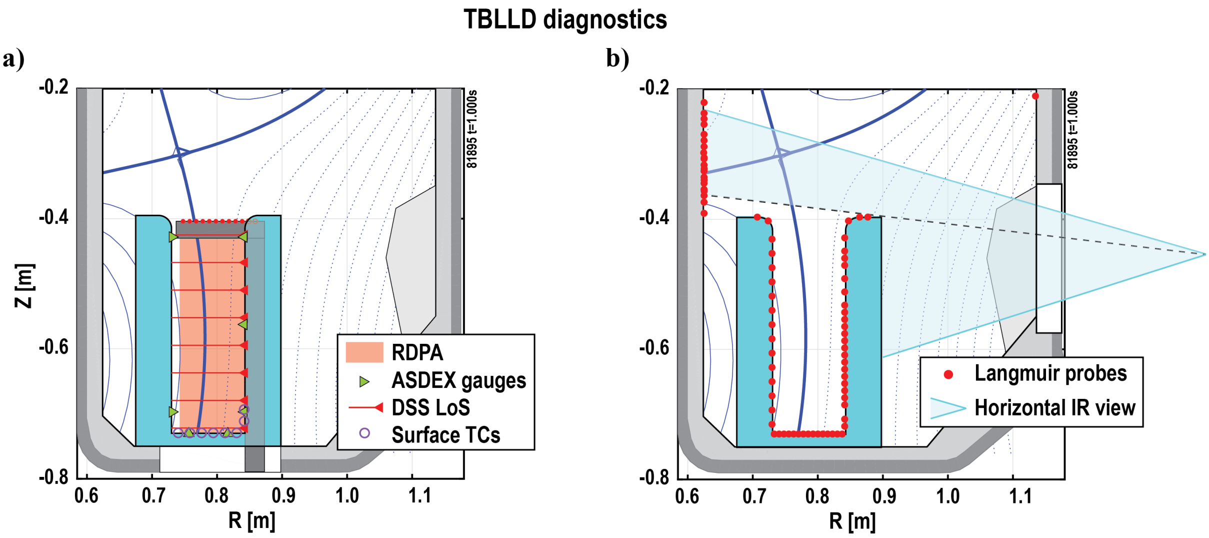

Figure 6. TBLLD diagnostics probing (a) the outer divertor and (b) also the inner target.

The TBLLD must not interfere with key core measurements, in particular those that characterise core performance. A small recess in an outer baffle tile will allow the laser used for Thomson scattering (TS) measurements to pass, Figure 7, thereby, preserving the acquisition of core electron temperature and density profiles [26]. Line integrated measurements of the electron density will be obtained from the interferometer, Figure 7. While the TBLLD baffles will block four of its 14 chords, six will intersect the low-field side radius of the core without intersecting the divertor and four the high-field side radius also sampling the TBLLD divertor volume (as mentioned above), Figure 7. Similar to accommodating the TS laser, the most central interferometer chord also requires a, somewhat larger, recess in outer baffle tiles. Measurements of the core ion temperatures using charge-exchange recombination spectroscopy (CXRS) as well as core radiation measurements with bolometers, AXUV and SXR diodes are not or only weakly affected by the TBLLD.

While further plasma characterisation, including most notably bolometric radiation measurements in the TBLLD volume, would be highly desirable, the set described herein should suffice to meet the objectives of the first phase of the TBLLD project.

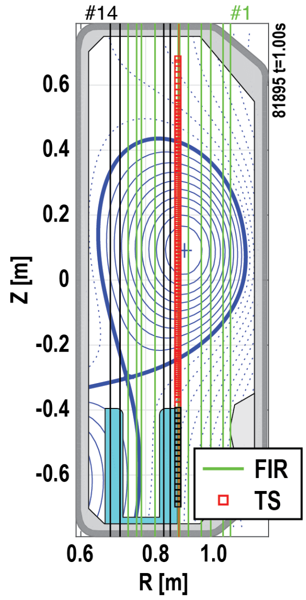

***Figure** 7. Compatibility with core diagnostics including measurements that are not available during the TBLLD campaign (black lines and symbols).*

6 CONCLUSIONS

The first phase of the next divertor upgrade of the TCV tokamak seeks to provide a proof-of-principle of the TBLLD concept. To this end, the outer divertor leg will be tightly baffled along the maximum length that is compatible with substantial NBI heating of the core. SOLPS-ITER predicts that the planned divertor will lead to significant increase of the power exhaust performance. Uncertainties in the predictions can be mitigated by varying the flux expansion and, thereby, the plasma plugging. The engineering design of the planned in-vessel structures, based on graphite tiles, benefits from the experience gained from the first generation TCV baffles, but pays greater attention to gas tightness. The foreseen diagnostic coverage of the TBLLD will be sufficient to detect and quantify these changes and, thereby, test the predictions and contribute to the physics basis of the TBLLD concept.

The application of the TBLLD concept solely to the outer divertor bears the risk that a large plasma temperature difference between the inner and outer targets will lead to a thermoelectric current that significantly affects the power distribution, removing power rather than dissipating it in the TBLLD and, thereby, jeopardising the proof-of-principle experiments. Such behaviour was seen in TCV simulations of TBLLD2, albeit at even higher input power than used in [8].

The procurement of all essential items has commenced and it is planned to the test the TBLLD in a dedicated experimental campaign in 2026. Concurrently, plasma-edge models are being used to extrapolate the TBLLD performance to a reactor-class device. Following a successful validation of the TBLLD concept, a second phase of the research infrastructure upgrade would aim at the exploration of an optimised baffle geometry, that also includes a solution for the inner divertor, addresses the problem of particle exhaust through the inclusion of a pump, e.g. as proposed in [27], and is compatible with an attractive core scenario, such as negative triangularity plasma shapes [28].

Acknowledgements

This work has been carried out within the framework of the EUROfusion Consortium, partially funded by the European Union via the Euratom Research and Training Programme (Grant Agreement No 101052200 — EUROfusion). The Swiss contribution to this work has been funded by the Swiss State Secretariat for Education, Research and Innovation (SERI). Views and opinions expressed are however those of the author(s) only and do not necessarily reflect those of the European Union, the European Commission or SERI. Neither the European Union nor the European Commission nor SERI can be held responsible for them. This work was supported in part by the Swiss National Science Foundation.

References

[1] C. Theiler, et al., *Progress and innovations in the TCV tokamak research programme*, this conference.
[2] M.V. Umansky, et al., Phys. Plasmas 24 (2017) 056112.
[3] H. Reimerdes, et al., Nucl. Fusion 60 (2020) 066030.
[4] M. Wigram, et al., Nucl. Fusion 59 (2019) 106052.
[5] A. Kallenbach, et al., Nucl. Fusion 55 (2015) 053026.
[6] R.A. Pitts, et al., Nucl. Mater. Energy 20 (2019) 100696.
[7] X. Bonnin, et al., Plasma Fusion Res. 11 (2016) 1403102.
[8] G. Sun, et al., Nucl. Fusion 63 (2023) 096011.
[9] H. De Oliveira et al., Rev. Sci. Instrum. 92 (2021) 043547.
[10] T. Body, et al., Nucl. Mater. Energy 41 (2024) 101819.
[11] E. Tonello, et al., *Modelling divertor solutions for power exhaust: in-depth experimental validation in TCV*, this conference.
[12] D. Vaccaro, et al., Fusion Eng. Des. 146 (2019) 1543.
[13] G. Sun, EPFL thesis No. No. 11103 (2025).
[14] A. Fasoli, et al., Nucl. Fusion 60 (2020) 016019.
[15] M. Baquero-Ruiz, et al., Fusion Eng. Des. 165 (2021) 112267.
[16] G. Sun, et al., Rev. Sci. Instrum. 96 (2025) 083502.
[17] B. Brown, et al., *Interpretation of Neutral Pressure Measurements and Design of a Novel Pressure Diagnostic Array for the TCV Tokamak through Monte Carlo Modelling with MolFlow*, Joint annual meeting of APS and SPS 2025, Vienna, Austria.
[18] A. Perek, et al., Rev. Sci. Instrum. 90 (2019) 123514.
[19] H. De Oliveira, et al., Rev. Sci. Instrum. 90 (2019) 083502.
[20] D. Brunner, B. LaBombard, Rev. Sci. Instrum. 83 (2012) 033501.
[21] R. Maurizio, et al., Nucl. Fusion 58 (2018) 016052.
[22] H. De Oliveira, et al., Rev. Sci. Instrum. 92 (2021) 043547.
[23] L. Martinelli, et al., Rev. Sci. Instrum. 93 (2022) 123505.
[24] R. Ducker, et al., *High-resolution visible spectroscopy for ion temperature and flow velocity measurements of the TCV divertor plasma*, submitted to Rev. Sci. Instrum.
[25] S. Barry, et al., Rev. Sci. Instrum. 67 (1996) 1814.
[26] P. Blanchard, et al., JINST 14 (2019) C10038.
[27] J. Yu, et al., Nucl. Mater. Energy 41 (2024) 101826.
[28] O. Février, et al., *Core-edge integration studies in Negative Triangularity in TCV*, this conference.